SUPPLEMENTAL INFORMATION

Contains: Figure S1, Table S1, Figure S2, Figure S3, analytical solution to seven-component fit and references.

Figure S1.

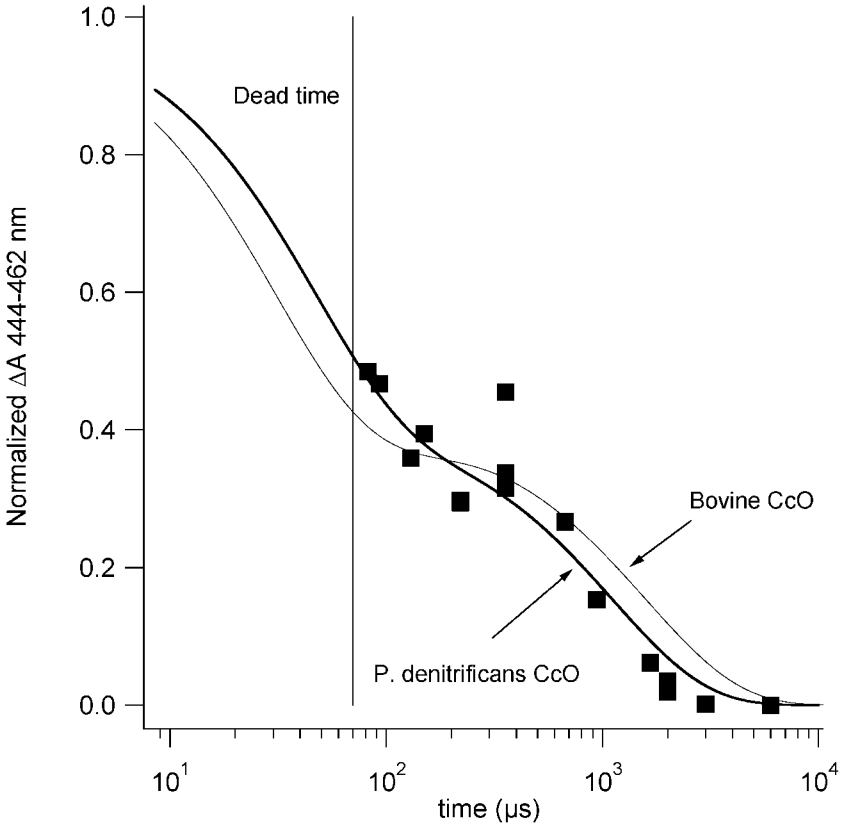

Figure S1. Normalized absorbance change at 444 - 462 nm (squares) representing the time course of oxidation of hemes (a+a_3) calculated from the low temperature UV-Vis spectra of Fig. 1. The simulations (thick line for the *P. denitrificans* CcO) are four-exponential fits exactly as in (S1), with the parameters summarized in Table S1. The relative spectral contributions determined for the bovine heart CcO (S1) were used for the *P. denitrifcans* CcO. The initial oxidation of the hemes is apparently faster in the bovine heart enzyme, while the second oxidation phase is faster in the *P. denitrificans* CcO (Table S1).

Table S1 Simulated half-lives for the oxidation of (heme a+a_3)

Transitions	**R → A**	**A → P_R**	**P_R → F**	**F → O_H**
Spectral contribution at 444-462 nm[1)]	b_1 0.363	b_2 0.327	b_3 -0.106	b_4 0.415
P. denitrificans CcO $t_{1/2}$	31.3 μs	34.3 μs	48.9 μs	776 μs
Bovine CcO[1)] $t_{1/2}$	15.9 μs	24.3 μs	65.9 μs	1109 μs

[1)] See ref (S1) for the meaning and values of the $b_{1\text{-}4}$ coefficients.

Figure S2.

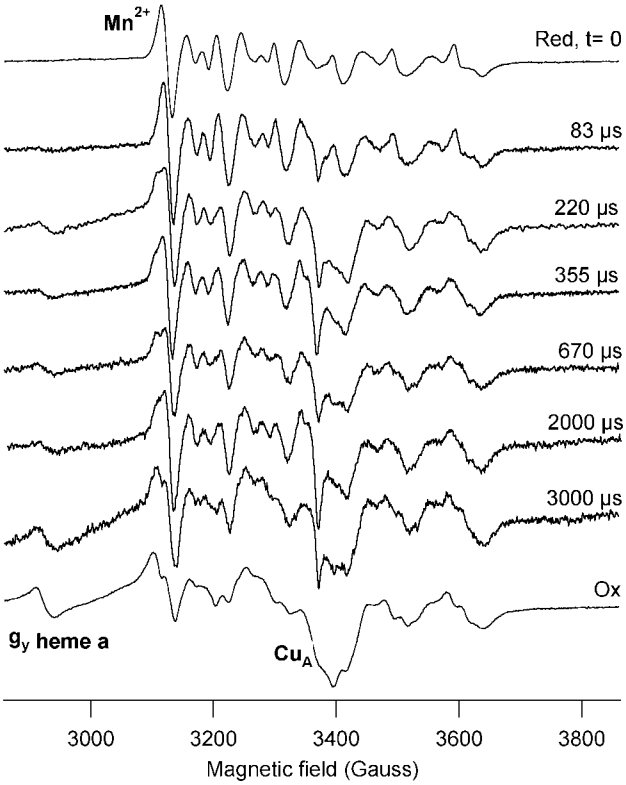

Figure S2. Representative X-band EPR spectra of Mn^{2+}-containing cytochrome aa_3 from *P. denitrificans* rapidly mixed with O_2 and reacted for various times (indicated in µs).
The g_y-resonance of heme *a* and the $g_\perp$ of Cu_A corrected for the Mn^{2+} contribution were used to determine their redox states. Expansion of the g=2 region (not shown) allowed estimation of the Trp* concentration though less accurate than in the Mn^{2+}-free samples. Some of these data are, however, also plotted in Figure 6. EPR conditions: Frequency: 9.42 GHz; modulation amplitude: 1.0 mT; microwave power: 2 mW; Temperature: 14 K. The spectra are normalized correcting for differences in gain and enzyme concentrations.

Figure S3.

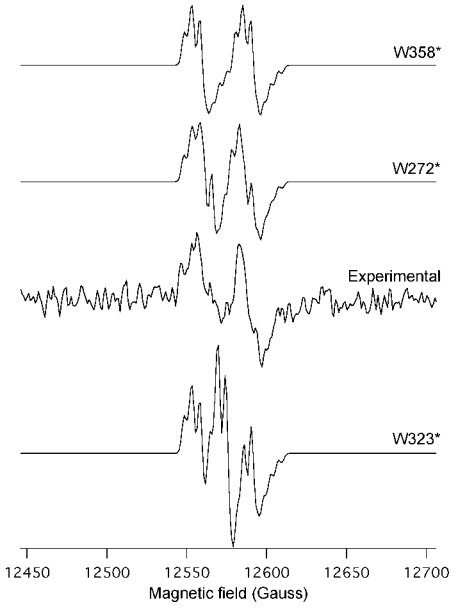

Figure S3. Experimental Q-band EPR spectrum (as in Figure 4) and simulations of specific Trp* radicals. For W328* and W358* all simulation parameters were the same as for W272* (Table 1) except the values for the β-methylene protons. For W358*: $H\beta_1$= 16; $H\beta_2$=16. For W325*: $H\beta_2$= 32; $H\beta_1$=0.

Analytical solution for a series of six irreversible sequential reactions.

The formation and decay rates of the reaction sequence $\mathbf{R \rightarrow A \rightarrow P_M \rightarrow P_R \rightarrow F \rightarrow F_{W^*} \rightarrow O_H}$ can be calculated by solving a set of seven differential equations. Analytical solutions for three or four components have appeared in textbooks (e.g. (S2)) and in the literature (e.g. (S1)), respectively. The basic calculation strategy described in these references was extended to seven components. The mathematical expressions below were used to simulate the traces in Figures 5, 6, and 8.

Define: A_0 = [R] at t=0 and $\alpha=1/((k_1-k_2)*(k_1-k_3)*(k_4-k_1))$; $\beta=1/((k_1-k_2)*(k_2-k_3)*(k_4-k_2))$; $\gamma=1/((k_1-k_3)*(k_2-k_3)*(k_4-k_3))$.

The expressions are written according to computer-programming language rather than to mathematical convention.

$\mathbf{R}=A_0*(\exp(-k_1*x))$

$\mathbf{A}=A_0*(((-k_1)/(k_1-k_2))*(\exp(-k_1*x)) + ((k_1)/(k_1-k_2))*(\exp(-k_2*x)))$

$\mathbf{P_M}=A_0*(((k_1*k_2)/((k_1-k_2)*(k_1-k_3)))*(\exp(-k_1*x))-((k_1*k_2)/((k_1-k_2)*(k_2-k_3)))*(\exp(-k_2*x))+((k_1*k_2)/((k_1-k_3)*(k_2-k_3)))*(\exp(-k_3*x)))$

$\mathbf{P_R}=A_0*(k_1*k_2*k_3)*\exp(-k_4*x)*((1/((k_1-k_2)*(k_1-k_3)*(k_4-k_1)))*(\exp((k_4-k_1)*x)-1)-(1/((k_1-k_2)*(k_2-k_3)*(k_4-k_2)))*(\exp((k_4-k_2)*x)-1)+(1/((k_1-k_3)*(k_2-k_3)*(k_4-k_3)))*(\exp((k_4-k_3)*x)-1))$

$\mathbf{F}=A_0*(k_1*k_2*k_3*k_4)*(\alpha*((\exp(-k_1*x)-\exp(-k_5*x))/(k_5-k_1)+(\exp(-k_5*x)-\exp(-k_4*x))/(k_5-k_4))-\beta*((\exp(-k_2*x)-\exp(-k_5*x))/(k_5-k_2)+(\exp(-k_5*x)-\exp(-k_4*x))/(k_5-k_4))+\gamma*((\exp(-k_3*x)-\exp(-k_5*x))/(k_5-k_3)+(\exp(-k_5*x)-\exp(-k_4*x))/(k_5-k_4)))$

$P\alpha=\alpha*((\exp(-k_1*x)-\exp(-k_6*x))/((k_6-k_1)*(k_5-k_1))+(\exp(-k_6*x)-\exp(-k_5*x))/((k_5-k_1)*(k_6-k_5))+(\exp(-k_5*x)-\exp(-k_6*x))/((k_5-k_4)*(k_6-k_5))+(\exp(-k_6*x)-\exp(-k_4*x))/((k_6-k_4)*(k_5-k_4)))$

$P\beta=-\beta*((\exp(-k_2*x)-\exp(-k_6*x))/((k_6-k_2)*(k_5-k_2))+(\exp(-k_6*x)-\exp(-k_5*x))/((k_5-k_2)*(k_6-k_5))+(\exp(-k_5*x)-\exp(-k_6*x))/((k_5-k_4)*(k_6-k_5))+(\exp(-k_6*x)-\exp(-k_4*x))/((k_6-k_4)*(k_5-k_4)))$

$P\gamma=\gamma*((\exp(-k_3*x)-\exp(-k_6*x))/((k_6-k_3)*(k_5-k_3))+(\exp(-k_6*x)-\exp(-k_5*x))/((k_5-k_3)*(k_6-k_5))+(\exp(-k_5*x)-\exp(-k_6*x))/((k_5-k_4)*(k_6-k_5))+(\exp(-k_6*x)-\exp(-k_4*x))/((k_6-k_4)*(k_5-k_4)))$

$\mathbf{F_{W^*}}= A_0*(k_1*k_2*k_3*k_4*k_5)*(P\alpha+P\beta+P\gamma)$

$\mathbf{O_H} = A_0 - \mathbf{R} - \mathbf{A} - \mathbf{P_M} - \mathbf{P_R} - \mathbf{F} - \mathbf{F_{W^*}}$

Or to check for the correctness of the expressions:

$\mathbf{O_H} = k_6*\int \mathbf{F_{W^*}}.dt$

Reduced (Cu_A + heme *a*)= $A_0*(1 - 0.5*(\mathbf{P_R}+\mathbf{F} +\mathbf{F_{W^*}}) - \mathbf{O_H})$

Substitution of the half-lives ($t_{1/2}$= ln2/k) given below, reproduces the traces in Figure 8.

Transitions	$\mathbf{R \rightarrow A}$	$\mathbf{A \rightarrow P_M}$	$\mathbf{P_M \rightarrow P_R}$	$\mathbf{P_R \rightarrow F}$	$\mathbf{F \rightarrow F_{W^*}}$	$\mathbf{F_{W^*} \rightarrow O_H}$
P. denitrificans CcO $t_{1/2}$	16 µs	32 µs	.001 µs	27 µs	1200 µs	60 µs

REFERENCES SUPPLEMENTAL INFORMATION

S1 Szundi, I., Cappuccio, J., and Einarsdottir, O. (2004) *Biochemistry* **43**(50), 15746-15758

S2 Fersht, A. (1999) *Structure and Mechanism in Protein Science. A Guide to Enzyme Catalysis and Protein Folding*, W.H. Freeman and Company, NY